

# LONG-TERM STABILITY OF NIST CHIP-SCALE ATOMIC CLOCK PHYSICS PACKAGES

S. Knappe<sup>1</sup>, V. Shah<sup>2</sup>, V. Gerginov<sup>3</sup>, A. Brannon<sup>4</sup>,  
L. Hollberg<sup>1</sup>, and J. Kitching<sup>1</sup>

<sup>1</sup>NIST, Time and Frequency Division, Boulder, CO 80305

<sup>2</sup>Department of Physics, University of Colorado, Boulder, CO 80309

<sup>3</sup>Department of Physics, University of Notre Dame, Notre Dame, IN 46556

<sup>4</sup>Department of Elec. Eng., University of Colorado, Boulder, CO 80309

## Abstract

*We present measurements regarding the long-term frequency stability of NIST chip-scale atomic clock (CSAC) physics packages. Changes of the clock frequency are caused mainly through time-dependent light shifts by the frequency-modulated VCSEL and properties of the vapor cell. We suggest advanced CPT interrogation schemes to relax the requirements on the temperature stability of the VCSEL as well as the power of the local oscillator. Finally, we discuss the advantages and limitations of these techniques when implemented into a small package.*

## INTRODUCTION

Chip-scale atomic clocks (CSACs) [1] have been an active field of research for only the past 4 years. CSAC physics packages have been demonstrated with short-term frequency instabilities of  $4 \times 10^{-11} / \tau^{1/2}$  [2]. Low-power devices have been developed consuming less than 10 mW in a package smaller than 1 cm<sup>3</sup> [3]. Low-power local oscillators [4] have also been developed and integrated with miniature physics packages [5]. Small prototypes that integrate the physics package, local oscillator, and control electronics have been demonstrated with volumes below 10 cm<sup>3</sup> and with power consumptions below 150 mW [6].

One of the major advantages of atomic timekeeping is its potential to achieve extremely good frequency stability over long time periods. In commercially available rubidium vapor cell clocks, the major source of instability is related to cell temperature drift [7, 8] and long-term buffer gas composition [9,10], optical and RF power changes, external magnetic fields, and aging of various components. Some of these issues have been addressed by simply steering the output frequency to compensate for frequency drifts, while others have been compensated for by more advanced physics setups, or minimized by additional electronic servos (for a tutorial on commercial rubidium standard technology, see for example [11]).

Chip-scale atomic clocks can potentially achieve good long-term frequency stability, and have the added advantages of low cost and low power dissipation, in addition to small size. To reach the goal of good long-term frequency stability, methods similar to those developed for larger clocks could be used, but the

additional requirements of low power consumption and low cost can place tighter constraints on the use of materials and engineering. Furthermore, it might be undesirable to add complicated frequency steering electronics. Some commercial rubidium frequency standards implement digital temperature compensation, for example by storing a table of frequency corrections for many temperatures [11]. These limitations point to the increased importance of addressing frequency drifts by use of advanced physics setups and servos. The major components in the CSAC that are not found in most conventional atomic clocks are the microfabricated vapor cell, the low-power local oscillator, and the laser. Currently, the control of the laser appears to be the most critical component in determining the long-term performance of the CSAC.

Figure 1 shows the Allan deviations of several CSAC subsystems constructed at NIST. CSAC physics packages based on  $^{87}\text{Rb}$  excited on the  $D_1$  line can support a frequency stability of  $4.5 \times 10^{-11} / \tau^{-1/2}$ , as shown in the black squares of Figure 1 [2]. When the CSAC physics package is integrated with a low-power local oscillator (the free-running stability of which is given by the green diamonds in Figure 1) [4], instabilities of  $2.4 \times 10^{-10} / \tau^{-1/2}$  have been measured (orange dots in Figure 1) [5]. Despite their good short-term stability, most of these devices show long-term instabilities on the order of  $10^{-9}$  at 1 day of integration. This paper discusses the reasons for these instabilities and suggests ways for improvement.

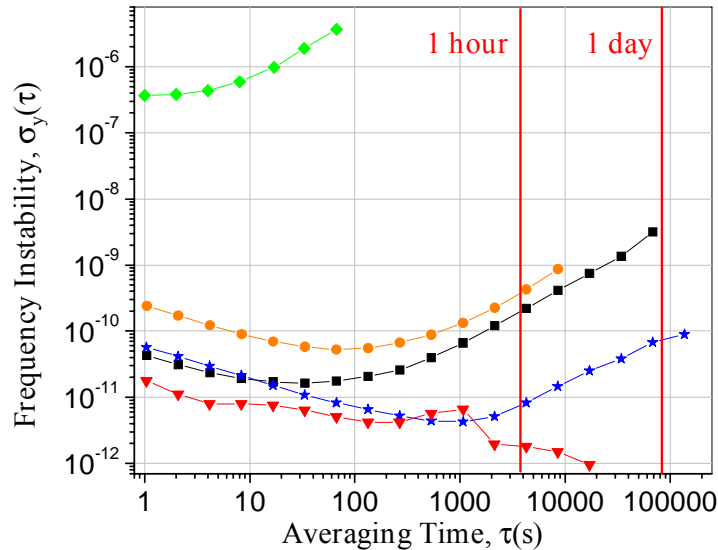


Figure 1. Allan deviation plots for a CSAC physics package (black squares), a low-power local oscillator free-running (green diamonds) and integrated with a CSAC physics package (orange dots), a microfabricated  $^{87}\text{Rb}$  vapor cell (blue stars), and a VCSEL CPT clock when locked to the point of minimum light shift (red triangles).

## CELL TEMPERATURE

In the first microfabricated vapor cells [12], two chemicals were reacted inside the cell cavities to produce the  $^{87}\text{Rb}$  atoms and nitrogen buffer gas. It was suspected that the residue of this reaction slowly depleted the nitrogen buffer gas, which resulted in clock frequency drifts around  $-2 \times 10^{-8}/\text{day}$  [13]. These drifts were largely eliminated by a new cell filling method with alkali deposition from a beam. Clocks based on

these cells have demonstrated clock frequency drifts to below  $5 \times 10^{-11}$ /day (mostly limited by our measurement system) [13]. Temperature coefficients of about  $10^{-9}$  per kelvin are easily achieved through the use of combinations of buffer gases with temperature coefficients of opposite sign [9,14]. This suggests that a cell temperature stability of 100 mK should be sufficient to achieve a clock stability of  $10^{-11}$ . The blue stars in Figure 1 show the fractional frequency stability measured in one such  $^{87}\text{Rb}$  vapor cell of interior volume  $1 \text{ mm}^3$ . It can be seen that the frequency stability at 1 hour is below  $10^{-11}$ . Currently, our CSACs are not limited by frequency shifts due to the vapor cells.

## VCSEL TEMPERATURE

One major difference between CSACs and conventional optically-pumped rubidium clocks is that CSACs use a low-power laser instead of a rubidium lamp to interrogate the atoms. Vertical-cavity surface-emitting lasers (VCSELs) have been chosen for their low threshold currents, vertical designs, and high modulation bandwidths. To excite coherent population-trapping (CPT) resonances [15], the VCSEL is usually modulated at half the clock frequency (a few gigahertz) [16]. This modulation creates a comb of optical sidebands around the fundamental laser frequency. The laser current and temperature are then tuned such that the frequencies of the two first-order modulation sidebands are in resonance with the transitions from the ground-state hyperfine levels to the excited state. When the second harmonic of the modulation frequency is exactly equal to the ground-state splitting of the  $m_F=0$  levels, the absorption of the first-order sidebands by the atoms is reduced, and this reduction can be observed by monitoring the optical power of the light transmitted through the atomic vapor. Finally, the laser modulation frequency can be stabilized to this atomic resonance and serves as the output of the clock.

It is well known that the transition frequency of alkali atoms in the vapor is perturbed by the resonant or near-resonant frequency components in the spectrum of the light source [9,17,18]. In CPT clocks based on modulated lasers, all sidebands of the frequency comb can shift the clock frequency [19]. Therefore, it is important that the sum of the AC Stark shifts from all the comb teeth does not change. The total power of the light field is determined by the VCSEL current, and the center frequency depends on both the VCSEL current and the VCSEL temperature. The frequency difference between the other modulation sidebands is determined by the modulation frequency of the LO. The relative power in each sideband is determined by the FM and AM modulation indices of the optical spectrum, which is in turn determined by the RF power of the LO and the extent to which this power is coupled into the VCSEL. Since the clock frequency shift depends critically on all of these parameters that might even change with time, the VCSEL temperature and current and the LO power have to be stabilized very well. For some of the NIST devices, temperature changes of the VCSEL can shift the clock frequency by  $\sim 5 \times 10^{-9}$ /K. This would mean that a 2 mK temperature stability would be required to maintain a clock frequency stability of  $10^{-11}$ . We believe that these instabilities can be largely reduced by better thermal design of the physics packages (e.g., vacuum packaging), as has been demonstrated by Lutwak *et al.* [3]. Nevertheless, we tried to investigate the causes for the frequency shifts of the NIST Physics packages in more detail to determine whether there are fundamental limitations to reaching instabilities of  $10^{-11}$  over longer times.

In the conventional CSAC setup, the laser temperature is monitored with a temperature sensor, e.g., a thermistor, in the vicinity of the VCSEL die. The laser frequency is stabilized to the top of the optical absorption resonance by slightly modulating the VCSEL current (at a few kilohertz rate) and by phase-sensitive detection of this modulation after transmission of the light through the cell. The laser current is then adjusted to maintain a stable laser frequency, but usually with a different output power. Part of the clock frequency shift is due to this change in total laser power as the laser temperature changes. Figure 2 displays a schematic of a conventional CSAC setup. It has been shown that this type of shift can be

minimized by choosing an RF modulation index such that the light shifts from all frequency sidebands cancel [19-21].

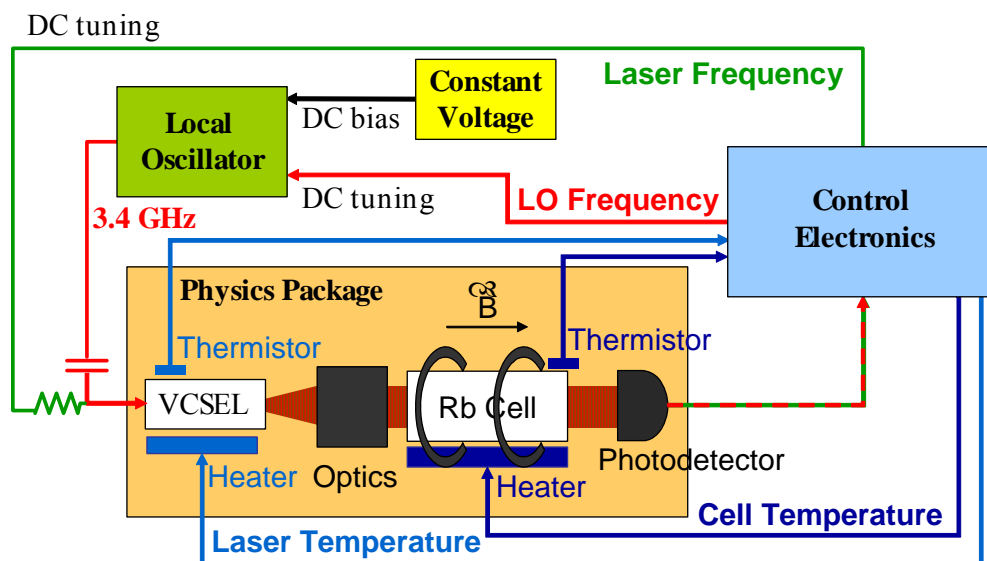


Figure 2. Schematic of a conventional CSAC setup consisting of a physics package, a local oscillator, and control electronics. Cell and VCSEL temperatures are stabilized by use of thermistors. The LO bias is supplied by a constant voltage source. The VCSEL frequency is locked to the top of the optical absorption line by modulating the VCSEL current and feeding the error signal, derived from the photodetector signal, back to it. The LO frequency is stabilized to the CPT resonance by modulation of the LO frequency and feeding the error signal derived from the photodetector signal back to the tuning port of the LO.

In normal operation, if the laser current changes, the impedance of the VCSEL can change simultaneously. This means that both the total power of all sidebands and the distribution of power among the sidebands, i.e., the modulation index, vary. Figure 3 (black symbols) shows the clock frequency shift as a function of VCSEL temperature for a series of RF powers. For this VCSEL, it can be seen that the modulation index can again be chosen such that the two effects compensate each other, and the total clock frequency shift is minimized [22, 23]. Unfortunately, this “magic” point depends on the individual VCSEL used, and the clock stability is not always optimal when operating at this point. To reduce production costs, a method that maintains this condition automatically and over a wide range of temperatures would be preferable. If the local oscillator is integrated with the VCSEL, we found that care must be taken so that the RF output power of the LO does not vary if the VCSEL impedance changes, because reflections back into the LO can alter the modulation index of the light even more severely.

Two approaches to reduce these problems have been investigated. In the first approach, very stable VCSEL output power, VCSEL frequency, and RF modulation index were maintained by use of signals directly derived from the alkali atoms directly [24]. While this method gave better frequency stability than the conventional technique at durations of an hour, further investigations to quantify the performance and limitations of this method are required. Therefore, an alternative approach is described, where the

modulation index of the light field is actively stabilized to the point where the clock frequency is independent of laser temperature [23].

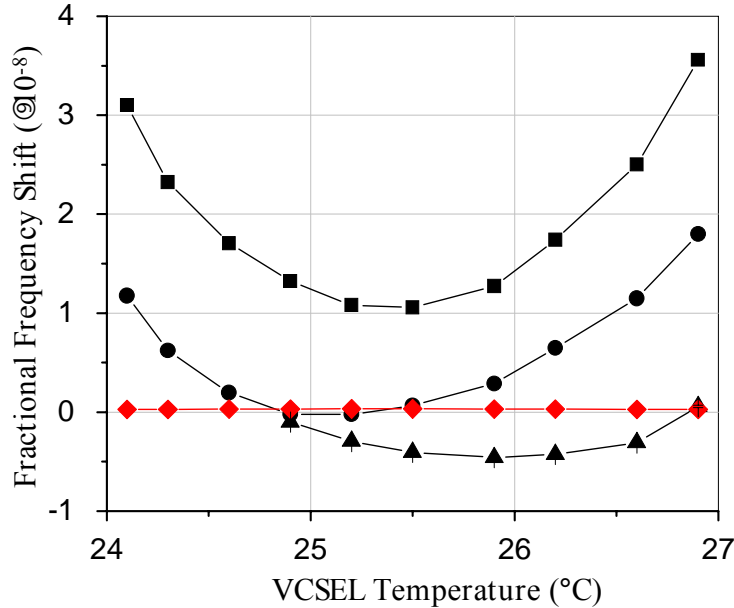


Figure 3. Fractional frequency shift of the CPT clock as a function of VCSEL temperature. The black symbols correspond to RF powers of -3.25 dBm (squares), -1.44 dBm (dots), and -0.75 dBm (triangles), respectively. The red diamonds correspond to the case when the RF power is tuned such that the light-shift modulation vanishes [23].

In order to stabilize the clock frequency to the point where all light shifts vanish, the VCSEL power was slowly modulated with an LCD attenuator [23]. In the presence of light shifts, the CPT resonance frequency was modulated in phase with the light power. This modulation was detected with a lock-in amplifier and displayed a zero-crossing when the RF power was chosen such that the total light shift vanished (see Figure 4). The error signal from the lock-in amplifier was used to actively stabilize the RF power so that the zero-crossing of the light shift was maintained under changes of the laser temperature. At the same time, the laser current was locked to the top of the optical resonance to maintain a constant laser frequency. The fractional frequency shift as a function of laser temperature under locked conditions can be seen in Figure 3 (red symbols).

This method was used to determine the long-term frequency stability that can be expected with the VCSELs. In order to not be limited by frequency drifts of the cell, a conventional glass-blown <sup>87</sup>Rb vapor cell was well temperature-stabilized and not in thermal contact with the VCSEL. The Allan deviation under such conditions can be seen as the red triangles in Figure 1 [23]. Frequency stabilities well below 10<sup>-11</sup> can be supported this way over many hours of integration. The short-term stability when operating with this second lock was degraded by only a factor of 1.2 for the VCSELs used. Nevertheless, other VCSELs can have modulation characteristics that make it less favorable to work at the point of no light residual shift. In a small CSAC setup, this could be easily implemented by varying the VCSEL

temperature to servo the LO bias in order to stabilize the clock to the point of no light shift. Furthermore, this is possible without major design changes of the existing CSAC physics packages.

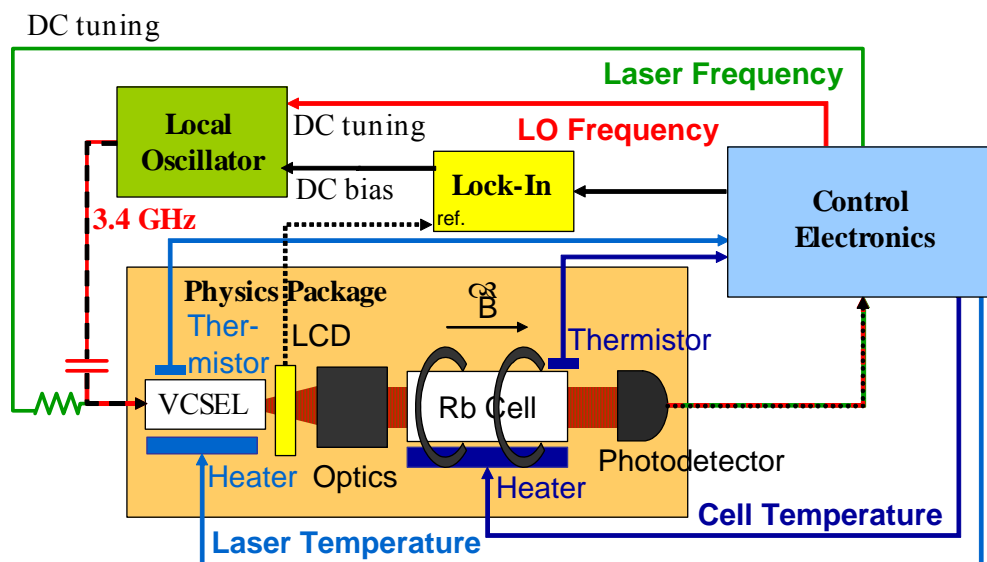


Figure 4. Schematic of a CSAC based on the method of locking to the point of no light shift. Here, cell and VCSEL temperatures are stabilized by use of thermistors. The VCSEL frequency is locked to the top of the optical absorption line by modulating the VCSEL current and feeding the photodetector error signal back to it. The LO frequency is stabilized to the CPT resonance by modulating the LO frequency and feeding the error signal, derived from the photodetector signal, back to the tuning port of the LO. The modulation index is chosen to the point where the modulation on the optical power does not cause a modulation in the CPT resonance frequency. This is done by modulating the light power with an LCD modulator and feeding the CPT error signal derived from the photodetector signal into a second lock-in detector. This second error signal is then used to tune the LO bias.

## CONCLUSION

We present measurements of microfabricated vapor cells and VCSELs in CPT clock setups that can support frequency instabilities below  $10^{-11}$  at 1 hour of integration. We suggest spectroscopic schemes that could aid in reaching such long-term frequency stabilities in miniature CSAC physics packages. We have so far found no fundamental reasons that would prevent CSACs from reaching frequency stabilities of around  $10^{-11}$  at one hour of integration.

## ACKNOWLEDGMENTS

We thank the Microsystems Technology Office of the U.S. Defense Advanced Research Projects Agency for financial support. A. Brannon is grateful for funding from a graduate research fellowship from the

National Science Foundation. This work is a contribution of NIST, an agency of the U.S. government, and is not subject to copyright.

## REFERENCES

- [1] S. Knappe, V. Shah, P. D. D. Schwindt, L. Hollberg, J. Kitching, L. A. Liew, and J. Moreland, 2004, "A microfabricated atomic clock," **Applied Physics Letters**, **85**, 1460-1462.
- [2] S. Knappe, P. D. D. Schwindt, V. Shah, L. Hollberg, J. Kitching, L. Liew, and J. Moreland, 2005, "A chip-scale atomic clock based on Rb-87 with improved frequency stability," **Optics Express**, **13**, 1249-1253.
- [3] R. Lutwak, J. Deng, W. Riley, M. Varghese, J. Leblanc, G. Tepolt, M. Mescher, D. K. Serkland, K. M. Geib, and G. M. Peake, 2005, "The Chip-Scale Atomic Clock – Low-Power Physics Package," in Proceedings of the 36th Annual Precise Time and Time Interval (PTTI) Systems and Applications Meeting, 7-9 December 2004, Washington, D.C., USA (U.S. Naval Observatory, Washington, D.C.), pp. 339-354.
- [4] A. Brannon, J. Breitbarth, and Z. Popović, 2005, "A Low-Power Low Phase Noise Local Oscillator for Chip-Scale Atomic Clocks," in Proceedings of the 2005 IEEE MTT-S International Microwave Symposium, 12-15 June 2005, Long Beach, California, USA (IEEE).
- [5] A. Brannon, V. Gerginov, S. Knappe, Z. Popović, and J. Kitching, 2006, "System-level integration of a chip-scale atomic clock: microwave oscillator and physics package," in Proceedings of the 1st Annual Multiconference on Electronics and Photonics, 7-11 November 2006, Guanajuato, Mexico, in press.
- [6] R. Lutwak, P. Vlitias, M. Varghese, M. Mescher, D. K. Serkland, and G. M. Peake, 2005, "The MAC – A Miniature Atomic Clock," in Joint Meeting of the IEEE International Frequency Control Symposium and the Precise Time and Time Interval (PTTI) Systems and Applications Meeting, 29-31 August 2005, Vancouver, Canada (IEEE 05CH37664C), pp. 752-757.
- [7] J. C. Camparo, C. M. Klimcak, and S. J. Herbulock, 2005, "Frequency equilibration in the vapor-cell atomic clock," **IEEE Transactions on Instrumentation and Measurement**, **IM-54**, 1873-1880.
- [8] M. Bloch, O. Mancini, and T. McClelland, 2000, "Performance of rubidium and quartz clocks in space," in Proceedings of the 2000 IEEE/EIA International Frequency Control Symposium & Exhibition, 7-9 June 2000, Kansas City, Missouri, USA (IEEE 00CH37052), pp. 505-509.
- [9] M. Arditi and T. R. Carver, 1961, "Pressure, Light, and Temperature Shifts in Optical Detection of 0-0 Hyperfine Resonance of Alkali Metals," **Physical Review**, **124**, 800-809.
- [10] J. Vanier, R. Kunski, P. Paulin, M. Têtu, and N. Cyr, 1982, "On The Light Shift In Optical-Pumping Of Rubidium 87 – The Techniques Of Separated And Integrated Hyperfine Filtering," **Canadian Journal of Physics**, **60**, 1396-1403.
- [11] W. Riley, "Rubidium Frequency Standard Technology, 2002, [www.ieee-uffc.org/freqcontrol/](http://www.ieee-uffc.org/freqcontrol/)

[tutorials/Riley\\_PTTI\\_2002.htm](#).

- [12] L. A. Liew, S. Knappe, J. Moreland, H. Robinson, L. Hollberg, and J. Kitching, 2004, “*Microfabricated alkali atom vapor cells*,” **Applied Physics Letters**, **84**, 2694-2696.
- [13] S. Knappe, V. Gerginov, P. D. D. Schwindt, V. Shah, H. Robinson, L. Hollberg, and J. Kitching, 2005, “*Atomic vapor cells for chip-scale atomic clocks with improved long-term frequency stability*,” **Optics Letters**, **30**, 2351-2353.
- [14] J. Vanier, R. Kunski, N. Cyr, J. Y. Savard, and M. Têtu, 1982, “On Hyperfine Frequency-Shifts Caused By Buffer Gases - Application To The Optically Pumped Passive Rubidium Frequency Standard,” **Journal Of Applied Physics**, **53**, 5387-5391.
- [15] G. Alzetta, A. Gozzini, L. Moi, and G. Orriols, 1976, “*Experimental-Method for Observation of Rf Transitions and Laser Beat Resonances in Oriented Na Vapor*,” **Nuovo Cimento della Societa Italiana di Fisica B-General Physics, Relativity, Astronomy, and Mathematical Physics and Methods**, **36**, 5-20.
- [16] N. Cyr, M. Têtu, and M. Breton, 1993, “*All-Optical Microwave Frequency Standard – A Proposal*,” **IEEE Transactions on Instrumentation and Measurement**, **IM-42**, 640-649.
- [17] J. P. Barrat and C. Cohen-Tannoudji, 1961, “*Etude du pompage optique dans le formalisme de la matrice densité*,” **Journal de Physique et le Radium**, **22**, 329-336.
- [18] B. S. Mathur, H. Tang, and W. Happer, 1968, “*Light Shifts in the Alkali Atoms*,” **Physical Review**, **171**, 11.
- [19] J. Vanier, A. Godone, and F. Levi, 1999, “*Coherent microwave emission in Coherent Population Trapping: Origin of the energy and of the quadratic light shift*,” in Proceedings of the Joint Meeting of the 13th European Frequency and Time Forum (EFTF) and the 1999 IEEE International Frequency Control Symposium, 12-16 April 1999, Besançon, France (IEEE), pp. 96-99.
- [20] F. Levi, A. Godone, and J. Vanier, 2000, “*Light shift effect in the coherent population trapping cesium maser*,” **IEEE Transactions on Ultrasonics, Ferroelectrics, and Frequency Control**, **47**, 466-470.
- [21] M. Zhu and L. S. Cutler, 2000, “*Theoretical and experimental study of light shift in a CPT-based Rb vapor cell frequency standard*,” in Proceedings of the 32nd Annual Precise Time and Time Interval (PTTI) Systems and Applications Meeting, 28-30 November 2000, Reston, Virginia, USA (U.S. Naval Observatory, Washington, D.C.), pp. 311-323.
- [22] V. Gerginov, S. Knappe, V. Shah, P. D. D. Schwindt, L. Hollberg, and J. Kitching, 2006, “*Long-term frequency instability of atomic frequency references based on coherent population trapping and microfabricated vapor cells*,” **Journal of the Optical Society of America B-Optical Physics**, **23**, 593-597.



- [23] V. Shah, V. Gerginov, P. D. D. Schwindt, S. Knappe, L. Hollberg, and J. Kitching, 2006, “*Continuous Light Shift Correction in Modulated CPT Clocks*,” **Applied Physics Letters**, in press.
- [24] V. Gerginov, V. Shah, S. Knappe, L. Hollberg, and J. Kitching, 2006, “*Atomic-based stabilization for laser-pumped atomic clocks*,” **Optics Letters**, **31**, 1851-1853.

